

## Spontaneous Formation of Nanosized Unilamellar Polyion Complex Vesicles with Tunable Size and Properties

Yasutaka Anraku,<sup>†</sup> Akihiro Kishimura,<sup>\*,†</sup> Makoto Oba,<sup>‡,§</sup> Yuichi Yamasaki,<sup>†</sup> and Kazunori Kataoka<sup>\*,†,‡,||,⊥</sup>

Department of Materials Engineering, Graduate School of Engineering, The University of Tokyo, 7-3-1 Hongo, Bunkyo-ku, Tokyo 113-8656, Center for Disease Biology and Integrative Medicine, Graduate School of Medicine, The University of Tokyo, 7-3-1 Hongo, Bunkyo-ku, Tokyo 113-0033, Department of Clinical Vascular Regeneration, Graduate School of Medicine, The University of Tokyo, 7-3-1 Hongo, Bunkyo-ku, Tokyo 113-8655, Center for NanoBio Integration, The University of Tokyo, 7-3-1 Hongo, Bunkyo-ku, Tokyo 113-8656, and CREST, Japan Science and Technology Agency, Sanbancho 5, Chiyoda-ku, Tokyo 102-0075, Japan

Received October 1, 2009; Revised Manuscript Received November 24, 2009; E-mail: kishimura@bmw.t.u-tokyo.ac.jp; kataoka@bmw.t.u-tokyo.ac.jp

**Abstract:** Fabrication of monodispersed, submicrometer-sized vesicles (nanosomes) that form through self-assembly possessing a thin and permeable membrane remains a significant challenge. Conventional fabrication of nanosomes through self-assembly of amphiphilic molecules often requires cumbersome processes using organic solvents combined with physical procedures (e.g., sonication, thermal treatment, and membrane filtration) to obtain unilamellar structures with a controlled size distribution. Herein, we report the first example of spontaneously formed submicrometer-sized unilamellar polyion complex vesicles (Nano-PICsomes) via self-assembly of a pair of oppositely charged PEG block anioner and homocationer in an aqueous medium. Detailed dynamic light scattering and transmission electron microscopic analysis revealed that vesicle sizes can be controlled in the range of 100–400 nm with a narrow size distribution, simply by changing the total polymer concentration. Also, each Nano-PICsome was composed of a uniform single PIC membrane, the thickness of which is around 10–15 nm, regardless of its size. Fluorescence correlation spectroscopy measurement verified that Nano-PICsomes were able to encapsulate water-soluble fluorescent macromolecules in the inner water phase and release them slowly into the exterior. Moreover, cross-linking of the vesicle membrane allows tuning of permeability, enhancement in stability under physiological conditions, and preservation of size and structure even after freeze-drying and centrifugation treatment. Finally, Nano-PICsomes showed a long circulation time in the bloodstream of mice. Precise control of the particle size and structure of hollow capsules through simple aqueous self-assembly and easy modification of their properties by cross-linking is quite novel and fascinating in terms of ecological, low-cost, and low-energy fabrication processes as well as the potential utility in the biomedical arena.

### Introduction

Fabrication of monodispersed, submicrometer-sized vesicles (nanosomes) that form through self-assembly possessing a thin and permeable membrane remains a significant challenge, although they are expected to have many potential applications.<sup>1–3</sup> Conventional fabrication of liposomes and polymersomes as nanosomes often requires cumbersome processes using organic solvents combined with physical procedures (e.g., sonication,

thermal treatment, and membrane filtration) to obtain unilamellar structures with a controlled size distribution. These limitations often raise concerns regarding cost-effective and up-scaled production, biocompatibility, and deterioration of loaded materials, particularly in biorelated applications.<sup>4,5</sup> There are only a few examples reported to date for the formation of unilamellar nanosomes with a polymer or lipid origin.<sup>6–18</sup> Nevertheless,

<sup>†</sup> Department of Materials Engineering, Graduate School of Engineering, The University of Tokyo.

<sup>‡</sup> Center for Disease Biology and Integrative Medicine, Graduate School of Medicine, The University of Tokyo.

<sup>§</sup> Department of Clinical Vascular Regeneration, Graduate School of Medicine, The University of Tokyo.

<sup>||</sup> Center for NanoBio Integration, The University of Tokyo.

<sup>⊥</sup> Japan Science and Technology Agency.

- (1) Wang, Y.; Xu, H.; Zhang, X. *Adv. Mater.* **2009**, *21*, 1–16.
- (2) Blanz, A.; Armes, S. P.; Ryan, A. J. *Macromol. Rapid Commun.* **2009**, *30*, 267–277.
- (3) Lensen, D.; Vriezema, D. M.; Van Hest, J. C. M. *Macromol. Biosci.* **2008**, *8*, 991–1005.

(4) Onaca, O.; Nallani, M.; Ihle, S.; Schenk, A.; Schwaneberg, U. *Biotechnol. J.* **2006**, *1*, 795–805.

(5) Nyin, H.; Routh, A. F. *Soft Matter* **2006**, *2*, 940–949.

(6) Holowka, E. P.; Pochan, D. J.; Deming, T. J. *J. Am. Chem. Soc.* **2005**, *127*, 12423–12428.

(7) Azzam, T.; Eisenberg, A. *Angew. Chem., Int. Ed.* **2006**, *45*, 7443–7447.

(8) Batzri, S.; Korn, E. D. *Biochim. Biophys. Acta* **1973**, *298*, 1015–1019.

(9) Saegusa, K.; Ishii, F. *Langmuir* **2002**, *18*, 5984–5988.

(10) Domazou, A. S.; Luisi, P. L. *J. Liposome Res.* **2002**, *12*, 205–220.

(11) Souza, T. P.; Stano, P.; Luisi, P. L. *ChemBioChem* **2009**, *10*, 1056–1063.

(12) Kaler, E. W.; Murthy, A. K.; Rodriguez, B. E.; Zasadzinski, J. A. N. *Science* **1989**, *245*, 1371–1374.

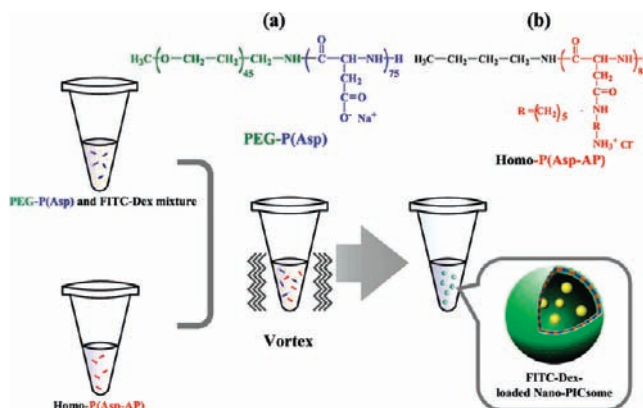
(13) Thomas, C. F.; Luisi, P. L. *J. Phys. Chem. B* **2004**, *108*, 11285–11290.

these processes often involve careful tuning of polymer structures, preformation of template vesicles, and the use of organic solvents, such as alcohol, to regulate the size of the vesicles on the nanometer length scale.

Recently, we reported the preparation of novel polymersomes by the simple mixing of water-soluble and oppositely charged block copolymers (block anionomers and block cationomers) composed of biocompatible poly(ethylene glycol) (PEG) and poly(amino acids) in an aqueous medium. The polymersome formed in this fashion is a new entity of polymeric vesicle consisting of a polyion complex (PIC) membrane sandwiched between outer and inner PEG shell layers, termed a "PICsome".<sup>19–21</sup> Compared with conventional vesicles, many advantages of PICsomes have been revealed so far, such as no need for an organic solvent, easy encapsulation of water-soluble macromolecules, semipermeability of the vesicle wall,<sup>19</sup> protease resistance,<sup>20</sup> and pH sensitivity.<sup>21</sup> Nevertheless, particle size control was difficult with PICsomes that spontaneously formed under physiological conditions as micrometer-sized particles (1–3  $\mu\text{m}$ ) with a relatively broad size distribution, which is common with other self-assembled vesicles from amphiphilic compounds. Moreover, these self-assembled vesicles usually do not have a well-defined unilamellar structure without any further processing. Hence, for broad applications in diverse biomedical fields such as drug delivery<sup>22–27</sup> and diagnostics,<sup>28–30</sup> a tighter control of vesicular structure at the submicrometer scale is key.

Herein, we report for the first time spontaneous formation of polymer-based nanosomes with a unilamellar permeable membrane and a narrow size distribution in an aqueous medium through polyion complexation of block ionomers. The size of these novel nanosomes with a unilamellar PIC membrane, termed "Nano-PICsomes", can be controlled in the range between 100 and 400 nm by simply changing the concentration of the oppositely charged ionomers in the reaction mixture. Furthermore, the cross-linking of the PIC membrane greatly

**Scheme 1.** Chemical Structures of Oppositely Charged Polymers for Nano-PICsomes and Schematic Representation of Nano-PICsome Preparation



improves the stability of the Nano-PICsomes against increased salt concentration in the medium as well as lyophilization and also modulates the solute transport to tune the permeability. Overall, these characteristics are highly encouraging for future biomedical applications as nanocarriers and nanoreactors.

## Results and Discussion

As previously reported, micrometer-sized PICsomes were obtained by mixing block anionomer PEG–poly( $\alpha,\beta$ -aspartic acid) (PEG–P(Asp);  $M_n$  of PEG 2000, DP of P(Asp) 75 (Scheme 1a)) and block cationomer PEG–poly([5-aminopentyl]- $\alpha,\beta$ -aspartamide) (PEG–P(Asp-AP);  $M_n$  of PEG 2000, DP of P(Asp-AP) 75) dissolved in 50 mM phosphate buffer (PB; 150 mM NaCl, pH 7.4).<sup>19–21</sup> Toward the control of the size and structure of PICsomes, we first examined the effect of the ionic strength, because it is well-known that the electrostatic interaction and hence the morphology of PICs are influenced by the ionic strength of the solution.<sup>31,32</sup> In fact, mixing of PEG–P(Asp) and PEG–P(Asp-AP) in the solution with reduced ionic strength (10 mM PB without NaCl, pH 7.4) gave spherical micelles with a diameter of around 40 nm instead of micrometer-sized PICsomes at a charge stoichiometric condition ( $-\text{COO}^-/-\text{NH}_3^+ = 1$ ) (Table 1, Figures 1a (dashed line) and S6 (Supporting Information)<sup>33</sup>) (total polymer concentration ( $C_{\text{pol}}$ ) = 1 mg/mL). Interestingly, transition from spherical micelles into Nano-PICsomes in the same buffer occurred by simply changing the partner of PEG–P(Asp) from PEG–P(Asp-AP) to the corresponding homocationomer Homo-P(Asp-AP) (DP of P(Asp-AP) 82 (Scheme 1b)). A clear shift in the average particle diameter from 40 to 100 nm was observed at the stoichiometric condition, keeping a narrow particle size distribution (Table 1 and Figure 1a, solid line). Detailed structural analysis with cryogenic phase contrast transmission electron microscopy (cryo-TEM) was completed after structural fixation by cross-linking (vide infra) (Figure 1b). Remarkably, the formation of Nano-PICsomes composed of a uniform membrane whose thickness is approximately 10–15 nm was observed under cryo-TEM. This value is less than the fully extended chain length of the constituent polyelectrolyte strands ( $\sim 18$  nm), roughly estimated by summation of the average backbone length unit (C–C–N, 0.24 nm). Thus, the observed and calculated membrane thickness

- (14) Kabanov, A. V.; Bronich, T. K.; Kabanov, V. A.; Yu, K.; Eisenberg, A. *J. Am. Chem. Soc.* **1998**, *120*, 9941–9942.  
 (15) Bronich, T. K.; Ouyang, M.; Kabanov, V. A.; Eisenberg, A.; Szoka, F. C., Jr.; Kabanov, A. V. *J. Am. Chem. Soc.* **2002**, *124*, 11872–11873.  
 (16) Wang, Y.; Han, P.; Xu, H.; Wang, Z.; Zhang, X.; Kabanov, A. V. *Langmuir* **2010**, *26*, 709–715.  
 (17) Zhang, Y.; Huang, W.; Zhou, Y.; Yan, D. *J. Phys. Chem. B* **2009**, *113*, 7729–7736.  
 (18) Guo, B.; Shi, Z.; Yao, Y.; Zhou, Y.; Yan, D. *Langmuir* **2009**, *25*, 6622–6626.  
 (19) Koide, A.; Kishimura, A.; Osada, K.; Jang, W.-D.; Yamasaki, Y.; Kataoka, K. *J. Am. Chem. Soc.* **2006**, *128*, 5988–5989.  
 (20) Kishimura, A.; Koide, A.; Osada, K.; Yamasaki, Y.; Kataoka, K. *Angew. Chem., Int. Ed.* **2007**, *46*, 6085–6088.  
 (21) Kishimura, A.; Liamsuwan, S.; Matsuda, H.; Dong, W.-F.; Osada, K.; Yamasaki, Y.; Kataoka, K. *Soft Matter* **2009**, *5*, 529–532.  
 (22) Gabizon, A. *Clin. Cancer Res.* **2001**, *7*, 223–225.  
 (23) Torchilin, V. P. *Nat. Rev. Drug Discovery* **2005**, *4*, 145–160.  
 (24) Ahmed, F.; Pakunlu, R. I.; Srinivas, G.; Brannan, A.; Bates, F.; Klein, M. L.; Minko, T.; Discher, D. E. *Mol. Pharmaceutics* **2006**, *3*, 340–350.  
 (25) Holowka, E. P.; Sun, V. Z.; Kamei, D. T.; Deming, T. J. *Nat. Mater.* **2007**, *6*, 52–57.  
 (26) Khalil, I. A.; Kogure, K.; Futaki, S.; Hama, S.; Akita, H.; Ueno, M.; Kishida, H.; Kudoh, M.; Mishina, Y.; Kataoka, K.; Yamada, M.; Harashima, H. *Gene Ther.* **2007**, *14*, 682–689.  
 (27) Peer, D.; Karp, J. M.; Hong, S.; Farokhzad, O. C.; Margalit, R.; Langer, R. *Nat. Nanotechnol.* **2007**, *2*, 751–760.  
 (28) Ghoroghchian, P. P.; Frail, P. R.; Susumu, K.; Blessington, D.; Brannan, A. K.; Bates, F. S.; Chance, B.; Hammer, D. A.; Therien, M. J. *Proc. Natl. Acad. Sci. U.S.A.* **2005**, *102*, 2922–2927.  
 (29) Lecommandoux, S.; Sandre, O.; Chécot, F.; Rodriguez-Hernandez, J.; Perzyski, R. *Adv. Mater.* **2005**, *17*, 712–718.  
 (30) Krack, M.; Hohenberg, H.; Kornowski, A.; Linder, P.; Weller, H.; Förster, S. *J. Am. Chem. Soc.* **2008**, *130*, 7315–7320.

- (31) Abe, K.; Ohno, H.; Tsuchida, E. *Makromol. Chem.* **1977**, *178*, 2285–2293.  
 (32) Dautzenberg, H. *Macromolecules* **1997**, *30*, 7810–7815.  
 (33) See the Supporting Information.

**Table 1.** DLS Analysis of PIC Assemblies Prepared from Different Combinations at Various Concentrations

combination of polymers	concn ( $C_{\text{pol}}$ , mg/mL)	size (mean $\pm$ SEM) <sup>a,b</sup> (nm)	polydispersity index
PEG-P(Asp)/ PEG-P(Asp-AP)	1	39.0 $\pm$ 1.10	0.051 $\pm$ 0.011
PEG-P(Asp)/ Homo-P(Asp-AP)	0.1	100 $\pm$ 1.60	0.041 $\pm$ 0.012
	0.5	99.3 $\pm$ 3.20	0.048 $\pm$ 0.012
	1	100 $\pm$ 1.40	0.023 $\pm$ 0.016
	2	155 $\pm$ 3.70	0.037 $\pm$ 0.012
	3	218 $\pm$ 11.9	0.041 $\pm$ 0.014
	4	244 $\pm$ 14.3	0.042 $\pm$ 0.010
	5	310 $\pm$ 12.5	0.051 $\pm$ 0.015
	7	344 $\pm$ 16.3	0.078 $\pm$ 0.010
	10	387 $\pm$ 21.7	0.078 $\pm$ 0.013

<sup>a</sup> Standard error of the mean (SEM) ( $n = 3$ ). <sup>b</sup> Each value was calculated using the cumulant method.

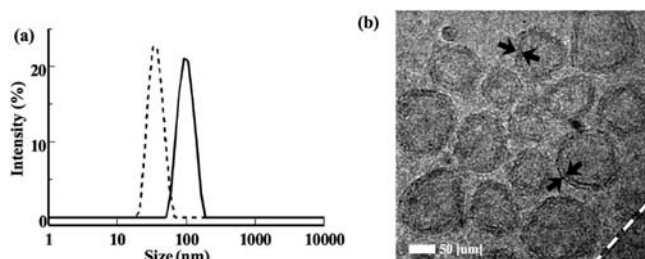


**Figure 1.** (a) Representative size distributions of PIC assemblies prepared from PEG-P(Asp) and PEG-P(Asp-AP) (dashed line) and PEG-P(Asp) and Homo-P(Asp-AP) (Nano-PICsomes, solid line) determined by DLS. The total polymer concentration is 1 mg/mL. (b) Representative cryo-TEM image of Nano-PICsomes after cross-linking treatment. Arrows are placed to underline vesicle walls. The white dashed line shows a contour of the microgrid.

is consistent with the formation of the unilamellar structure, provided that the polymer strands in the PIC do not possess a fully extended conformation because of the reduced electrostatic repulsion through polyion complexation.

The replacement of the block cationer PEG-P(Asp-AP) with the homocationer Homo-P(Asp-AP) brings a drastic change in the self-assembly scheme from micelle to vesicle. Here, we assume that a reduction in PEG weight fraction ( $f_{\text{PEG}}$ ) from  $\sim 15\%$  in the block anioner/block cationer system to  $\sim 8\%$  in a block anioner/homocationer system may increase the stability of the lamellar phase due to the decreased steric repulsion of the PEG shell layer.<sup>34–36</sup> This assumption is consistent with our previous observation that the partial detachment of the PEG strands from the PIC micelles induced in situ transition of the micelles into vesicles, in which a PEG fraction of  $<10\%$  is a key for vesicle formation.<sup>36</sup> Furthermore, a lower ionic strength condition might enable tight packing of a PIC and consequent requisite stability against high curvature and bending energies. This view is plausible because PICsomes with micrometer size were only found in the presence of 150 mM NaCl for both block anioner/block cationer and block anioner/homocationer systems (Figure S7, Supporting Information<sup>33</sup>).<sup>19–21,37</sup> Conse-

quently, the  $f_{\text{PEG}}$  and ionic strength are critical factors to determine the morphology and the size of PIC assemblies.

Unprecedentedly, we found that the size of Nano-PICsomes was tunable with keeping their unilamellar structure by changing the total polymer concentration,  $C_{\text{pol}}$ .  $C_{\text{pol}}$  was varied over 0.1–10 mg/mL, since enough scattering intensity for light scattering measurement was not obtained at concentrations  $<0.09$  mg/mL. In the range of  $C_{\text{pol}} > 1$  mg/mL, an increase in  $C_{\text{pol}}$  also increased the Nano-PICsome size (Table 1). The results showed a particle size increase from 100 to 387 nm while maintaining a PDI  $<0.1$ , which is indicative of a narrow size distribution. As shown in Figure 2, all Nano-PICsomes that were studied by cryo-TEM showed a unilamellar structure with particle sizes consistent with dynamic light scattering (DLS) measurements. Figure 3 plots the  $C_{\text{pol}}$  against the square of average diameters as determined by DLS measurement; data points fall onto a straight line obtained by a least-squares method, thereby indicating that  $C_{\text{pol}}$  values of 0.1–10 mg/mL strongly correlate with the surface area of Nano-PICsomes. Succinctly stated, the polymer concentration controls the number of molecules that self-assemble into a single vesicle. This direct correlation can be explained by assuming that each of the Nano-PICsomes may emerge simultaneously in a confined unit space of constant volume within the solution: a behavior similar to solute nucleation upon phase separation. The number of polymer strands in the unit space proportionally increases with the concentration, thereby resulting in an increased surface area.

Judging from an almost constant size of 100 nm in the range of  $C_{\text{pol}} < 1$  mg/mL, 100 nm may be the lower critical size of the Nano-PICsomes formed from the present block anioner/homocationer pair, presumably determined by the structural confinement. This critical phenomenon in the size of the Nano-PICsome might be a direct result from the balance between the thermodynamical gain by the reduction of surface energy through enclosure of the PIC lamellae and the accompanying penalty due to the bending of PIC lamellae with high curvature and steric hindrance of PEG chains located on the inner interface of PIC lamellae. Note that this size minimization in Nano-PICsome is comparable to the minimum size of conventional polymersomes composed of amphiphilic block copolymers.<sup>7</sup>

To investigate the potential utility of Nano-PICsomes, the permeability of the PIC wall was evaluated. Encapsulation of fluorescein isothiocyanate-labeled dextran (FITC-Dex,  $M_n = 10\,000$ ) into the inner phase of the Nano-PICsomes was completed followed by ultrafiltration to remove excess FITC-Dex. FITC-Dex loading was confirmed by fluorescence correlation spectroscopy (FCS), according to the previous study by Rigler and Meier where they demonstrated encapsulation of fluorescent molecules into a nanocontainer system.<sup>38,39</sup> FCS can quantitatively discriminate free and object-associated fluorescence molecules from the difference in their diffusion coefficients, thereby giving the size and number of encapsulated fluorescent objects.<sup>40</sup> Parts a and b of Figure 4 show normalized autocorrelation curves and fluorescence intensity traces of free FITC-Dex solution (10 nM) (i) and FITC-Dex/Nano-PICsome solution (ii), respectively. Comparison of the normalized autocorrelation curves clearly shows that the fluorescence decay time of the FITC-Dex/Nano-PICsome system is much longer than that of

(34) Discher, D. E.; Eisenberg, A. *Science* **2002**, *297*, 967–973.

(35) Antonietti, M.; Förster, S. *Adv. Mater.* **2003**, *15*, 1323–1333.

(36) Dong, W.-F.; Kishimura, A.; Anraku, Y.; Sayan, C.; Kataoka, K. *J. Am. Chem. Soc.* **2009**, *131*, 3804–3805.

(37) Oana, H.; Kishimura, A.; Yonehara, K.; Yamasaki, Y.; Washizu, M.; Kataoka, K. *Angew. Chem., Int. Ed.* **2009**, *48*, 4613–4616.

(38) Rigler, R.; Mets, Ü.; Widengren, J.; Kask, P. *Eur. Biophys. J.* **1993**, *22*, 169–175.

(39) Rigler, P.; Meier, W. *J. Am. Chem. Soc.* **2006**, *128*, 367–373.

(40) Axthelm, F.; Casse, O.; Koppenol, W. H.; Nausier, T.; Meier, W.; Palivan, C. G. *J. Phys. Chem. B* **2008**, *112*, 8211–8217.



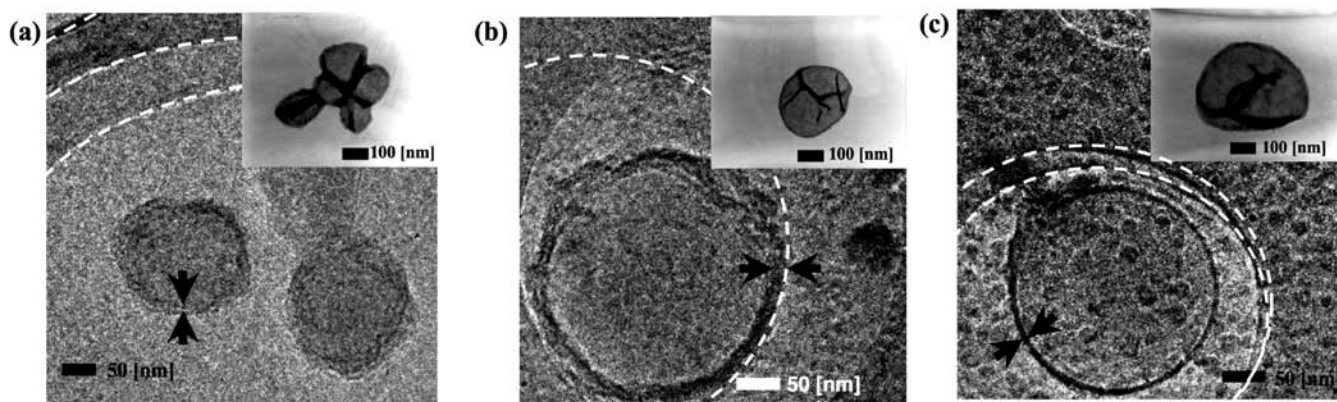


**Figure 2.** Representative images of PICsomes prepared at polymer concentrations of (a) 2 mg/mL, (b) 5 mg/mL, and (c) 10 mg/mL, obtained by cryogenic phase contrast TEM. Arrows are placed to underline vesicle walls. White dashed lines show a contour of the microgrid. Insets: conventional TEM images at each concentration.

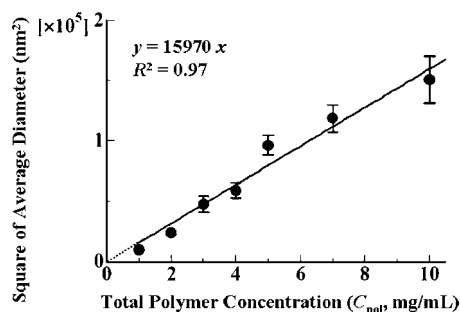


**Figure 3.** Total polymer concentration ( $C_{pol}$ ) against the square of the average diameters of the Nano-PICsomes.

free FITC–Dex, indicating the successful encapsulation of FITC–Dex into the Nano-PICosome (Figure 4a). Free FITC–Dex gave a constant drift in the intensity trace (Figure 4b(i)), whereas spikes in the fluorescence intensity trace of FITC–Dex/Nano-PICsomes were scattered (Figure 4b(ii)), indicative of the difference in the detection frequency between larger and smaller objects. Also, FITC–Dex/Nano-PICsomes show a significantly higher photon count rate (fluorescence intensity) than free FITC–Dex, indicating a highly effective FITC–Dex loading into each Nano-PICosome particle.

The permeability of FITC–Dex through the PIC wall of Nano-PICsomes was then examined by time-resolved FCS. The autocorrelation curve shifted to a shorter time region as time proceeded (Figure 4c). This result explicitly shows an increase in the fraction of FITC molecules with a higher diffusion coefficient, corresponding to the free FITC–Dex slowly releasing from the Nano-PICosome interior. Actually, curve ii measured at day 1 consists of two components with longer and shorter fluorescence decay times, explained as an overlay of the curves corresponding to the free FITC–Dex and Nano-PICosome-encapsulated FITC–Dex, respectively. At day 2, a constant and relatively low count rate was observed indicative of termination of FITC–Dex release (Figure S8, Supporting Information).<sup>33</sup> Moreover, all samples showed almost the same size and scattering intensity by DLS measurements (data not shown). These results clearly prove that FITC–Dex ( $M_n = 10\,000$ ) permeates the Nano-PICosome membrane in a sustained manner.

Notably, the cross-linking of the membrane allows Nano-PICsomes to acquire new functionality. Here, 1-ethyl-3-(3-(dimethylamino)propyl)carbodiimide hydrochloride (EDC) was used as a cross-linking reagent to form an amide bond from

the  $-\text{NH}_2$  and  $-\text{COOH}$  groups of the cationer and anioner, respectively. Even after the treatment of Nano-PICsomes with an excess amount of EDC, there was no appreciable change in the particle size as observed by DLS (Figure S9, Supporting Information).<sup>33</sup> Also, the preservation of the unilamellar structure was confirmed by cryo-TEM (Figures 2 and 3). Next, FITC–Dex ( $M_n = 10\,000$ ) permeability was checked using FCS in the aforementioned manner; the results showed a miniscule release of FITC–Dex even at day 2 (Figure 4d). This result promisingly suggests that, by varying the degree of cross-linking, the rate and extent of permeability may be finely controlled. Also, particle stability against physiological salt conditions was improved by this cross-linking treatment of the Nano-PICosome. After NaCl concentration adjustment to 150 mM NaCl, only cross-linked Nano-PICsomes retained a constant size as confirmed by the scattering intensity through DLS (Figure S10),<sup>33</sup> whereas Nano-PICsomes that were not cross-linked readily transformed into micrometer-sized objects (Figure S7).<sup>33</sup> Furthermore, cross-linked Nano-PICsomes retained their original particle size and distribution even after lyophilization (Figure S11)<sup>33</sup> as well as with centrifugal concentration (Figures 1b and S12).<sup>33</sup> Thus, the robustness of cross-linked Nano-PICsomes is of great advantage for practical applications, particularly in the pharmaceutical field as novel drug formulation materials.

Finally, we confirmed the utility of Nano-PICsomes as a long blood-circulating nanocarrier in *in vivo* experiments. Cy5–Nano-PICsomes (size 100 nm,  $\text{PdI} = 0.054$ ) were prepared from Cy5-labeled polyanion, PEG–P(Asp)–Cy5, and Homo-P(Asp-AP). After cross-linking treatment, Cy5–Nano-PICsomes were intravenously injected through the tail vein of BALB/c nude mice bearing murine colon 26 (C-26) adenocarcinoma sc tumors ( $n = 3$  except 120 h;  $n = 2$  at 120 h).<sup>33</sup> Cross-linked Cy5–Nano-PICsomes showed remarkably prolonged blood circulation, 14.5% of the initial dose remaining even after 48 h of injection, while both PEG–P(Asp)–Cy5 alone and Cy5–Nano-PICsomes without cross-linking were rapidly cleared from the bloodstream (Figure 5). It is noteworthy that the cross-linked Nano-PICsomes showed good longevity in the bloodstream which is comparable to that of typical long-lived liposomes and polymerosomes.<sup>41,42</sup> Accordingly, time-dependent accumulation of cross-linked Nano-PICsomes in C-26 tumor, evaluated by

(41) Photos, P. J.; Bacakova, L.; Discher, B.; Bates, F. S.; Discher, D. E. *J. Controlled Release* **2003**, *90*, 323–334.

(42) Blume, G.; Cevcec, G. *Biochim. Biophys. Acta* **1993**, *1146*, 157–168.

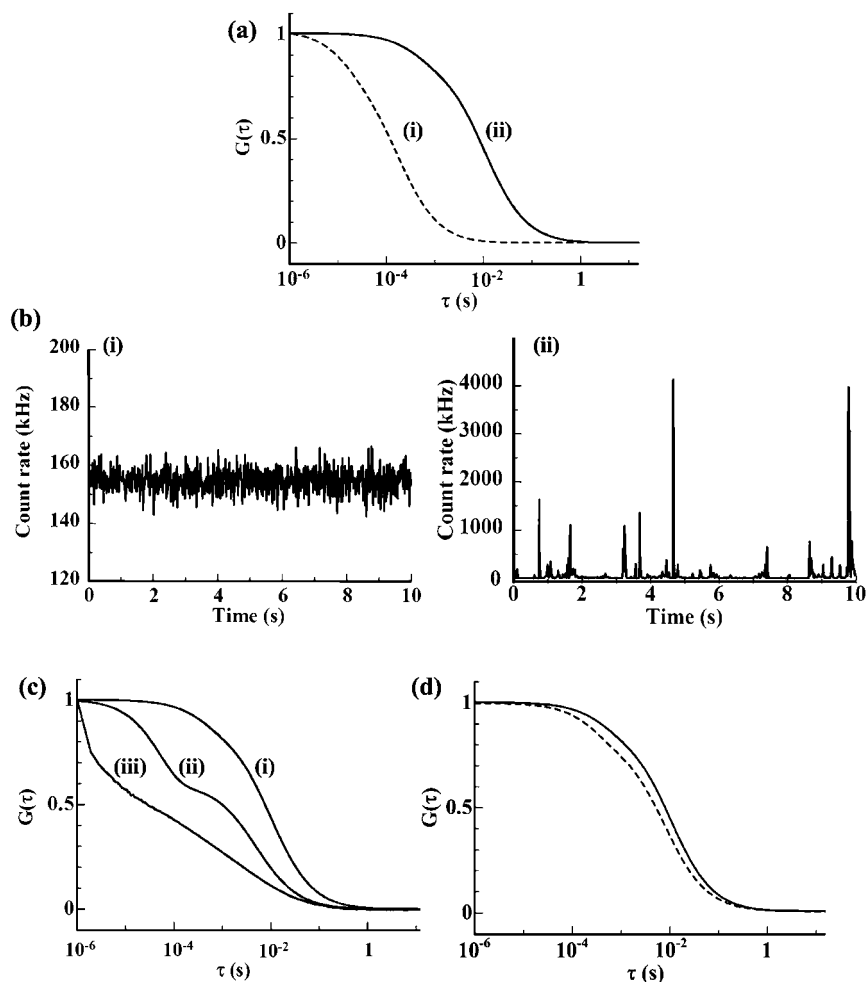


**Figure 4.** FCS analysis of free FITC-Dex and FITC-Dex-loaded Nano-PICsomes. (a) Normalized autocorrelation curves of free FITC-Dex (i, dashed line) and FITC-Dex-loaded Nano-PICsomes (ii, solid line). (b) Fluorescence intensity traces of free FITC-Dex (i) and FITC-Dex-loaded Nano-PICsomes (ii). [Free FITC-Dex] = 10 nM. (c) Time-resolved FCS analysis of FITC-Dex-loaded Nano-PICsomes. Each solid line shows a normalized autocorrelation curve obtained immediately after preparation (i), at day 1 (ii), and at day 2 (iii). (d) Time-resolved FCS analysis of FITC-Dex-loaded Nano-PICsomes after treatment with excess EDC. Each line shows normalized autocorrelation curves obtained immediately following preparation (solid line) and at day 2 (dashed line).

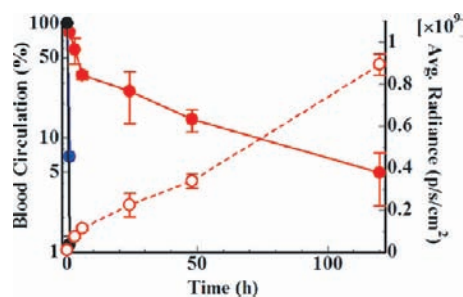


**Figure 5.** Plasma clearance of cross-linked Cy5-Nano-PICsomes (left axis, red closed circles), Cy5-Nano-PICsomes without cross-linking (black closed circles), and PEG-P(Asp)-Cy5 (blue closed circles). Time course of tumor accumulation of cross-linked Cy5-Nano-PICsomes evaluated by fluorescence imaging (right axis, open circles).

fluorescence imaging,<sup>33</sup> occurred as shown in Figure 5 due to the enhanced permeability and retention (EPR) effect.<sup>43</sup> This long circulation and enhanced tumor accumulation of

cross-linked Nano-PICsomes is promising for their future applications as smart nanocarriers of various bioactive compounds.

## Conclusion

The present study demonstrates the preparation of Nano-PICsomes, involving unilamellar structure and tunable size over 100–400 nm, through a remarkably simple method. Precise control of the size, distribution, and structure of nanometric scaled hollow capsules through self-assembly in an aqueous medium is quite novel and fascinating in terms of ecological, low-cost, and low-energy fabrication processes. Also, simple chemical modification, including cross-linking of the PIC layer, provides tunable permeability and stability in Nano-PICsomes. Finally, we found that cross-linked Nano-PICsomes attained an extremely long circulation property in the bloodstream. These outstanding features indicate the potential utility of Nano-PICsomes in the biomedical arena, such as artificial organelles, nanobioreactors, and nanocarriers of various diagnostic and therapeutic materials.

**Acknowledgment.** This research was supported in part by a Grant-in-Aid for Scientific Research (No. 19031003 to Y.Y., No.

(43) Matsumura, Y.; Maeda, H. *Cancer Res.* **1986**, *46*, 6387–6392.

21750166 to A.K., and No. 20•10495 to Y.A.) from the Ministry of Education, Culture, Sports, Science, and Technology (MEXT) of Japan and the Core Research Program for Evolutional Science and Technology from the Japan Science and Technology Agency. We are grateful to Dr. S. Fukuda, The University of Tokyo Hospital, for his valuable support in the TEM measurement, Drs. A. Kitayama and S. Sugitani, Terabase Inc., for cryo-TEM measurements, and Dr. K. Miyata, The University of Tokyo, for technical advice in the in vivo experiments. Y.A. thanks the JSPS Research Fellowship for Young Scientist. A.K. thanks the Inoue Foundation for Science, the Kao Foundation for Arts and Sciences, and the Izumi Science and Technology Foundation for financial support. We express our

appreciation to Dr. Darin Y. Furgeson (University of Utah) for proofreading this paper.

**Supporting Information Available:** Experimental Section, synthesis and characterization of polymers, TEM images of PIC micelles, a dark-field microscopic image, additional FCS diagrams, and additional particle size distributions of Nano-PICsomes. This material is available free of charge via the Internet at <http://pubs.acs.org>.

JA908350E